Physical processes in open discharge

A.P. Bokhan and P.A. Bokhan

Institute of Semiconductor Physics,
Siberian Branch of the Russian Academy of Sciences, Novosibirsk

Received November 27, 2001

Physical processes in an open discharge that are responsible for high efficiency of electron beam generation are studied. It is shown that effective e-beam generation is due to electron emission under conditions of UV irradiation and significant field distortion in an accelerating gap with simultaneous suppression of electron multiplication processes. The 99.8% practical efficiency of e-beam generation is achieved.

Introduction

Open discharge[1] (OD) arises in a narrow gap between a cathode and a perforated anode with an extended drift space behind it. Thanks to the capability of generating electron beams of keV energy with high efficiency, OD is a promising pump source for medium-pressure gas lasers.[2–5] However, OD itself is an object of intense studies. Nevertheless, in spite of two decades elapsed from the time of the first publications[6,7] and more than 100 papers devoted to this subject,[8] the main OD features and even its place among other discharges are, in essence, an open question. The main discussion questions, whose answers just determine the promises of OD usage, are the following:

1. Whether the photoemission from the drift space (DS) is a prevailing or at least significant channel of electron emission? In early papers, it was assumed that the photoemission is the main supplier of electrons to the beam current.[1,9,10] However, then this opinion was rejected in Refs. 11–14 for the mechanism of ion-electron emission, as in the abnormal discharge (AD) with e-beam.[15]

2. Whether the open discharge is a sort of the well-known abnormal discharge and, consequently, obeys its main laws, in particular, the volt-ampere characteristic (VAC) in He obeys the law[10]:

$$j/p^2 = 2.5 \cdot 10^{-10}\, U_c^3, \qquad (1)$$

where j is the current density; p is the gas pressure; U_c is the cathode voltage drop.

For the first time, the unusual VAC of the open discharge was noticed in Ref. 16. However, in Ref. 10 the conclusion was formulated that the open discharge VAC in a wide range of conditions obeys the law (1) and thus the open discharge is almost equivalent to the abnormal discharge. This sharply restricts the OD applicability because of intense cathode sputtering and impossibility of high-efficiency e-beam generation in the ordinary abnormal discharge at $p_{He} > 3$ Torr (Refs. 15, 17, and 18).

3. Where do electrons accelerate: in a narrow cathode region or in the entire accelerating gap (AG)? The available experimental papers on measuring the field in the accelerating gap[19–21] poorly agree with each other and with theoretical calculations.[5] At the same time, the character of the field distribution plays a very important role in the OD glow mechanism and in formation of its principal characteristics. With the close-to-uniform field distribution,[21] it is impossible to obtain $\eta \sim \mu$ (η is the efficiency, μ is the geometric transparency of a mesh anode), since it is known[22] that the mesh in this case intercepts the far larger part of the electron beam than it follows from the geometry. On the other hand, from the measurements in Ref. 19 it follows that in the dense OD $pl_0 \ll 0.37\, pl_n$. This contradicts the well-known relationship for the glow discharge $pl_a \geq 0.37\, pl_n$ (l_0, l_a, and l_n are, respectively, the length of the cathode voltage drop (CVD) region in the open, abnormal, and normal discharges). The inequality $pl_0 \ll 0.37\, pl_n$ allows, in principle, obtaining $\eta \sim \mu$, but immediately brings the OD out of the class of glow discharges.

Thus, the state of the art in the physics of the open discharge is not satisfactory. Revision of the already known results is needed, as well as new investigations which could help to overcome the above difficulties. Just this is the main subject of this paper.

1. Instrumentation and methods

Experimental studies were conducted in gas-discharge cells with an extra mesh.[23] This made it possible to independently control the emission from the drift space and to eliminate field sagging[24,25] to it.

Sets of identical cells with different lengths of the drift space and different areas of the cathode open part were used. This allowed the OD properties to be studied depending on the photoemission power, which is connected with the cathode diameter, and the glow area in the drift space by the equation:

$$I_s = \frac{1}{2} I_0 \int_0^h \int_0^R \frac{rz}{(r^2 + z^2)^{\frac{3}{2}}} \int \mathrm{d}r\, \mathrm{d}z\,, \qquad (2)$$

where I_0 is the specific radiation intensity; R is the radius of the cathode open part; h is the length of the drift space.

0235-6880/02/03 190-12 $02.00

Two modes of the OD glow were mostly studied, namely, (1) continuous mode with the current density up to 5 mA/cm^2 and (2) quasi-continuous mode with the current density up to 1 A/cm^2 and duration of a rectangular pulse $\tau = 10$ μs and up to 10 A/cm^2 at $\tau = 1$ μs.

2. Electron photoemission in an open discharge

2.1. Effect of discharge in the drift space on open discharge properties

The available papers on the OD give no direct proof for existence of photoemission from the cathode under its exposure to VUV radiation from the drift space. To find such proof in this work, a continuous discharge, in which a collector served a cathode, was initiated in the drift space. Continuous voltage was applied to the accelerating gap, and the current in it was measured under different conditions.

In Fig. 1, we can see a complex dependence of the current in the gap on the voltage U_g applied to it. First, it should be noted that the current of the gas-filled diode is far lower than the current of the vacuum diode $j_g = 2.34 \cdot 10^{-6}\, l_g^{-2}\, U_g^{3/2}$ (curve *7*, l_g is the gap length) even at the voltage from 1 to 10 V, at which the photocurrent is still far from saturation and independent of the intensity of UV irradiation. This difference is especially large at a high He pressure. At the voltage $U_g = 50$–100 V the photocurrent enters the first stage of saturation, and its dependence on the irradiance becomes evident. However, at $U_g \geq 100$ V the probability of helium ionization by accelerated primary photoelectrons, as they cross the gap, becomes close to unity, what finally at $U_g = 400$ V leads to almost threefold increase of the current as compared with its value at the first plateau. At $U_g > 400$ V the diode current begins to decrease, and then at $U_g > 560$ V a sharp increase starts. The decrease can be explained by the passage of the energy region with the maximal electron multiplication value. According to the theory of runaway electrons developed in Ref. 26, running-away in He under these conditions begins with the voltage $U_g \sim 200$ V. At $U_g > 400$ V the effect of runaway electrons, including secondary electrons, whose number decreases, becomes so significant that it leads to decreasing VAC. However, at $U_g > 560$ V the penetration of beam electrons into the drift space and the excitation of the working gas by them become a considerable factor in UV irradiation, what leads to the increase of the current. This stage has a pronounced breakdown character in the voltage region from 570 to 600 V. At $U_g \geq 600$ V the current in the accelerating gap evolves already by the laws of the open discharge.

The threshold field strength, at which an OD arises, is equal to $E/N = 1.67 \cdot 10^3$ TD, and at $E/N \geq 1.77 \cdot 10^3$ TD ($U_g > 600$ V) the discharge becomes a clearly pronounced OD (E is the field strength, N is the concentration of particles; 1 TD = 10^{-17} V · cm^2). In this case, it is not a self-sustaining OD, since shutdown of artificial irradiation or decrease of its power quenches the discharge in the accelerating gap. The self-sustaining OD glows at $E/N > 2.5 \cdot 10^3$ TD.

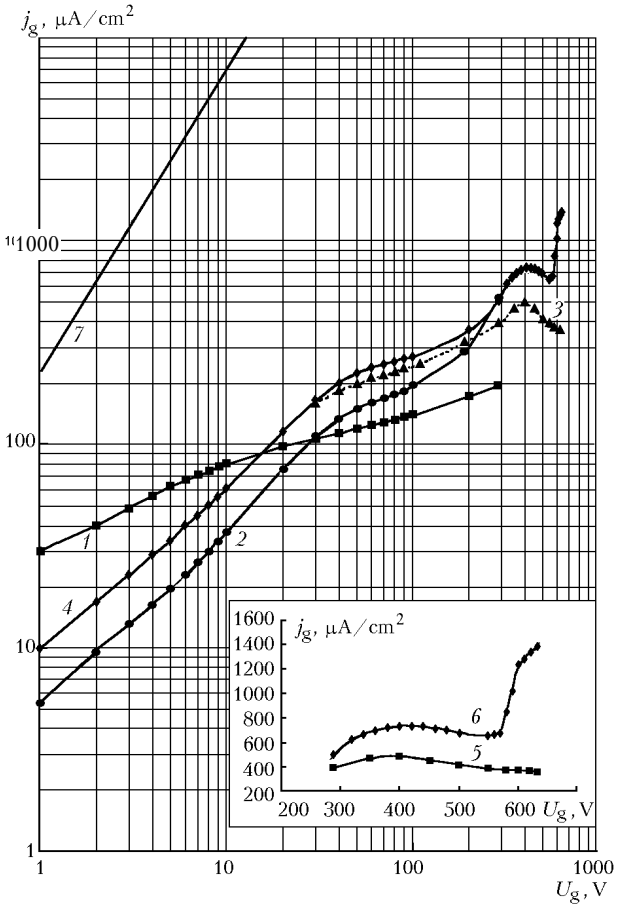

Fig. 1. Voltage dependence of the current density in the gap: $p_{He} = 5$ and 15.5 Torr (*1* and *2*) and $p_{He} = 9.6$ Torr (*3*–*6*); $I_d = 2.5$ mA (*1*–*3*, *5*) and $I_d = 7.5$ mA (*4*, *6*); I_d is the current in the drift space.

The obtained data directly prove the existence of considerable photoemission from the cathode of the accelerating gap due to UV illumination from the drift space. To study its effect on the OD characteristics in the cathode–anode gap with the mesh diameter $d_m = 12.5$ mm, continuous self-sustaining discharge was initiated in helium. For its stabilization, the ballast resistor R_b was connected in series. The measured parameters were the discharge current and the voltage across the accelerating gap. Then the constant voltage was applied to the second mesh – electron collector (EC) gap and the characteristics of the discharge in the accelerating gap were measured. The extensive studies under various conditions have shown that voltage application to the drift space always lead to the current increase in the accelerating gap. The corresponding data are partly presented in Ref. 23, and in more detail they will be reported in our next paper.

As an example, Fig. 2 shows the current in the accelerating gap in relation to its initial value $[(I_g/I_{g0}) \cdot 100\%]$ as a function of $(P_d/P_{e0}) \cdot 100\%$, where P_{e0} is the power scattered by fast beam electrons as they move in the drift space at $I = I_{g0}$, and P_d is the power of discharge in the drift space as calculated by the equation $P_d = U_d I_d$ (U_d and I_d are, respectively, the voltage applied to the drift space and the current of the non-self-sustaining discharge through it). The energy loss of keV-energy electrons was calculated based on the data of Refs. 5 and 27–29. It can be seen from Fig. 2 that the discharge in the drift space strongly affects the current in the accelerating gap. This effect can be caused only by photoemission, since the drift speed of ions from the drift space under the effect of the field is more than an order of magnitude lower than the thermal speed.[30]

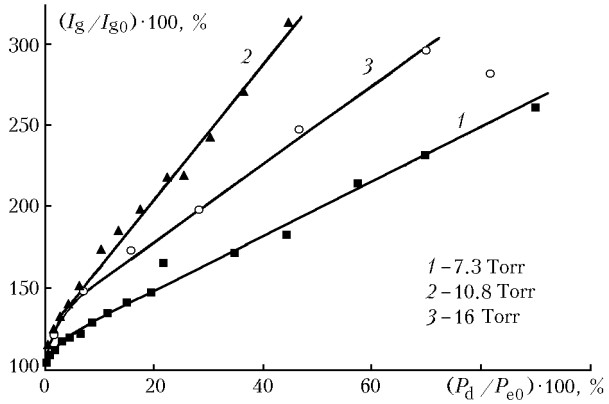

Fig. 2. Increase of the current in the gap vs. the relative power of discharge in the drift space: continuous mode (*1*, *2*) and quasi-continuous mode (*3*); I_{g0} = 1.5 mA (*1*, *2*) and 0.4 A (*3*).

2.2. Mechanisms of VUV radiation generation in open discharge

As it was shown above, the radiation generated in the OD affects the current in the accelerating gap and, consequently, electron emission from the cathode. It proceeds under the exposure to VUV radiation (VUV quanta) generated at transitions from the resonance and other excited atomic states to the ground state. The states are excited at collisions with beam electrons accelerated in the accelerating gap and entering the drift space, as well as due to the generation of electric fields accompanying the e-beam generation and propagation.[24,31] In He the mean energy of VUV quanta $h\nu_{He} \sim 22$ eV and in Ne $h\nu_{Ne} \sim 17.5$ eV. For this radiation, according to Refs. 32–37, the photoemission coefficient $\gamma_p = 0.15$–0.2 when using massive Al, Fe, Mo, Ta, or W cathodes in OD.

Finally, we are interested in the number of electrons $\gamma_{\Sigma p}$ emitted from the cathode under the effect of VUV quanta generated at deceleration of one electron. The condition for prevalence of photoemission and obtaining $\eta \sim \mu$ is fulfillment of the approximate equality $\gamma_{\Sigma p} \sim 1$. The parameter $\gamma_{\Sigma p}$ can be written as:

$$\gamma_{\Sigma p} = \gamma_p \mu (h\nu)^{-1} \sum_i \int (dE_i/dx)\, I_{si}(x) \eta_r(x) dx, \quad (3)$$

where dE_i/dx are energy losses of all types arising at beam propagation in the drift space; I_{si} is the geometric factor (2); η_r is the energy fraction consumed for excitation of the emitting atomic states in the working gas. The increase of γ_p at oblique incidence[33,38,39] was ignored. Let us consider the most important processes of generation of VUV radiation and estimate their contribution to $\gamma_{\Sigma p}$:

The parameter γ_{p1} is conditioned by direct energy losses of beam electrons at their motion in the medium as calculated based on the data of Refs. 5 and 28. According to Ref. 29, $\eta_r = 0.3$ at e-beam generation, and the remaining ~ 70% come for ionization. About 2/3 of excitation energy comes to the resonance state. More recent calculations[5] give ~ 51% for ionization and the rest for excitation. For Ne η_r is somewhat higher. Radiation trapping was also taken into account. In the continuous mode, as well as for Zn and Hg (Ref. 40), η_r is much higher thanks to recombination flux and equal to ~ 0.8;

The parameter γ_{p2} is conditioned by generation of induction and compensation currents[24,31] significantly decreasing the e-beam penetration depth. This effect can be easily taken into account based on the experimental data on the e-beam penetration depth.[41,42] In the discharge arising in this case $\eta_r = 0.5$ for He and $\eta_r = 0.6$ for Ne;

The parameter γ_{p3} is caused by field sagging in the drift space and excitation of the working gas in the non-self-sustaining discharge in this field. It plays a significant role only in continuous-wave beams and at the initial stage of a pulsed beam, when the field in the gap is not distorted by volume charges[19–21];

The parameter γ_{p4} is conditioned by inelastic and elastic scattering of fast electrons at the surface of the anode mesh[43–47] and excitation of the working gas by them;

The parameter γ_{p5} is conditioned by the secondary electron emission from the anode[43–45];

The parameter γ_{p6} is conditioned by excitation of the gas in the gap by electrons starting from the cathode and being at the acceleration stage, as well as the accelerating secondary electrons.

Table 1 presents the results of $\gamma_{\Sigma p}$ calculation for the typical examples of e-beam generation in OD in a wide range of conditions. To assess the applicability of the calculation technique, the last row presents the results on $\gamma_{\Sigma p}$ in the classical case of normal glow discharge in He (Ref. 49), $p_{He} = 2$ Torr, $d_c = 9.3$ cm, $l_g = 1.6$ cm. It can be seen from Table 1 that for the normal discharge $\gamma_{\Sigma p} = 0.066 \ll 1$ and photoemission contributes insignificantly to the electron emission. In all considered cases, $\gamma_{\Sigma p} > 1$ in OD, what confirms the conclusion on the considerable effect of photoemission on the electron emission at all stages and in all modes of the open discharge.

Table 1

#	l_g/h_d, mm	S_c, cm^2	Gas	p, Torr	Mode	U_g, kV	$j_g = I_g/s$, A/cm^2	γ_{p1}	γ_{p2}	γ_{p3}	γ_{p4}	γ_{p5}	γ_{p6}	$\gamma_{\Sigma p}$	$(I_i/I_e)\gamma_{\Sigma i}$	Ref.
	1	2	3	4	5	6	7	8	9	10	11	12	13	14	15	16
1	1/22	1.2	Ne	3.2	C	0.9	0.0015	0.67	—	0.09	0.09	0.04	0.16	1.05	0.04	t.p.
2	0.7/50	33	He	2.0	C	5.0	0.0133	0.43	—	> 0.8	—	—	—	> 1.2	0.04	48
3	1/22	1.2	He	10.6	C	1.12	0.001	0.63	—	0.09	0.08	0.04	0.28	1.12	0.07	t.p.
4	1/20	0.5	Ne	4.5	QC	2.46	0.41	0.42	—	0.25	0.15	0.10	0.25	1.17	0.03	19
5	0.5/50	0.8	He	30	P	5.8	30.6	0.17	0.61	—	0.21	—	0.13	1.12	0.03	24
5′	0.5/50	0.8	He	30	P	7.8	$< 10^{-2}$	0.15	—	0.96	0.27	0.19	0.13	1.7	0.02	24
6	1/50	1	Ne	7.5	P	3.8	30.0	0.36	2.08	—	0.17	—	0.42	3.03	—	42
7	1/30	1	Ne	2.2	QC	8.5	0.2	0.09	—	0.68	0.32	0.20	0.1	1.11	—	14
7′	4/30	1	Ne	2.2	QC	7.3	2.7	0.10	—	0.05	0.28	0.02	0.72	1.17	—	14
8	4.5/99	10^3	Ne	2.3	P	8	3.0	0.82	—	0.10	0.28	0.03	0.20	1.43	—	4
9	—	—	He	2.0	C	0.165	10^{-5}	0.03	—	—	0.01	—	0.026	0.066	—	49

Notes: C means continuous mode; QC means quasi-continuous mode; P means pulsed mode; t.p. is for this paper.

To determine whether photoemission is a decisive factor that determines the OD properties, we have to study the conditions of self-sustaining and their relation with the emission mechanism and reliably established main OD parameters, in particular, the efficiency of e-beam generation.

3. Efficiency of e-beam generation and its relation with the conditions of discharge self-sustaining and the mechanism of electron emission

The high efficiency of e-beam generation in OD, roughly equal to the geometric transparency of the anode mesh, imposes certain restrictions on fulfillment of the self-sustaining conditions and the mechanism of electron emission. For illustration, we analyze the already mentioned experiment from Ref. 24, which was considered in Refs. 12 and 14 as the typical for the pulsed open discharge and unexplainable from the viewpoint of the photoelectron mechanism. Figure 3 depicts the oscillograms of voltage U_g across the accelerating gap (*1*), e-beam current I_e (*2*), and anode current I_a (*3*) in He at the pressure of 4 kPa and the geometric transparency of the anode mesh $\mu = 0.75$. It can be seen from Fig. 3 that the efficiency of the e-beam generation behind the anode at the maximum e-beam current is

$$\eta = I_e/(I_e + I_a) = 22.4/(22.4 + 8.2) = 0.732. \quad (4)$$

Since a part of the beam is intercepted by the mesh, for physical investigations it is useful to apply the concept of the internal efficiency of e-beam generation in the gap η_{in} (Ref. 19), which is equal to η at $\mu \to 1$:

$$\eta_{in} = I_{e0}/I_e + I_a = I_e/(I_e + I_a)\ \mu = \eta/\mu, \quad (5)$$

where $I_{e0} = I_e/\mu$ is the e-beam current inside the gap. For the cited case $\mu = 0.75$ and $\eta_{in} = 0.976$.

Consider the restrictions imposed by $\eta_{in} = 0.976$ on the mechanism of electron emission. At photoemission, $\eta_{in} \sim 1$ is fulfilled automatically if $\gamma_{\Sigma p} > 1$ and the ion current to the cathode is low. The same is true for the self-sustaining condition. However, fulfillment of $\gamma_{\Sigma p} > 1$ still does not mean that, for example, a pulsed open discharge is a photoelectron one. It may turn out that every electron emitted from the cathode generates so many ions with such energy that the total emission under their effect is much higher than the photoemission, as in ordinary glow discharges. Therefore, it is necessary to estimate the contribution to electron emission at cathode bombardment by heavy particles.

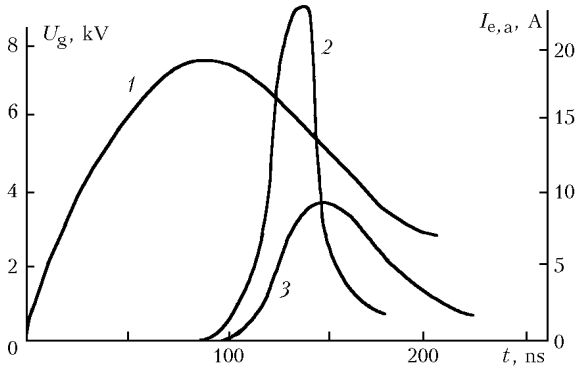

Fig. 3. Oscillograms of voltage across the cathode (*1*), e-beam current at the collector (*2*), and the current in the anode circuit (*3*) at $l_g = 0.5$ mm, $p_{He} = 4$ kPa, and the cathode area $S_c = 0.8$ cm^2 (Ref. 24).

3.1. Mechanism of ion-electron emission

To determine the contribution of the ion bombardment of the cathode to the electron emission, let us express the anode current through the e-beam current intercepted by the mesh and the current of secondary electrons in the gap that compensate the ion current to the cathode I_i:

$$I_a = I_{e0}\ (1 - \mu) + I_i. \quad (6)$$

It can be shown that

$$I_{e0}/I_i = \eta_{in}/1 - \eta_{in}, \quad (7)$$

and this leads to the value:

$$I_{e0}/I_i = 40.7. \quad (8)$$

Equation (8) means that every ion reaching the cathode should knock out ~ 41 electrons, i.e., the coefficient of ion-electron emission should be $\gamma_i \sim 41$. Actually, for the Al cathode used in Ref. 23, $\gamma_i \sim 0.48$ (Refs. 32 and 50), if $E_i = 6$ keV. This condition is fulfilled, when ions are accelerated at the length l_0 of the CVD region roughly equal to the ion mean free path before collision in the recharging reaction $l_0 \sim \lambda_c$ (Ref. 19) and the whole applied voltage U_g is concentrated within l_0. Thus, the actual coefficient of the ion-electron emission is two orders of magnitude lower than needed to explain the experimentally measured efficiency of the e-beam generation.

3.2. Mechanism of atom-electron emission

Ions are accelerated up to the energy $E_i \sim eU_g = 6$ keV only if $l_0 \sim \lambda_c$. At $l_0 > \lambda_c$ an ion acquires lower energy because of the loss during the reaction of resonance recharging. Consequently, γ_i decreases.[32,50] However, fast atoms are generated in the recharging reaction, and they also can cause the electron emission with the coefficient γ_a. Let us estimate this effect.

We still assume that the voltage drop is mostly concentrated in the cathode region, but its length can be arbitrary up to the CVD length of normal discharge.[51] As l_0 increases, the total electron emission $\gamma_{\Sigma i}$ per one ion reaching the cathode can be calculated by standard methods.[15,52] In calculations we took into account the data on γ_i at $E_i > 2$ keV from Refs. 32, 50, 53, and 54, at $E_i < 2$ keV from Refs. 55 and 56, and for γ_a from Refs. 38, 55, and 56. The recharging and elastic scattering cross sections were borrowed from Refs. 45 and 57–59 for helium and from Refs. 45, 59, and 60 for Ne. The plot obtained for He is depicted in Fig. 4. According to this plot, $\gamma_{\Sigma i}(\max) = \gamma_i + \Sigma\gamma_a = 0.72$. This value is far (~ 57 times) smaller than γ needed for fulfillment of Eq. (8).

3.3. Effect of the surface state on $\gamma_{\Sigma i}$

Because of pollution of the working gas and formation of surface layers on the cathode, $\gamma_{\Sigma i}$ in actual beam experiments may be much higher than that depicted in Fig. 4 (Refs. 38, 52, and 61–63). Therefore, in e-beam generators based on abnormal discharge under the conditions of technological vacuum, the efficient $\gamma_{\Sigma i}$ is calculated from the ratio of the power transferred by e-beams to the power scattered at the cathode.[15] The obtained empiric dependence has the form $\gamma_{\Sigma i} \sim 0.2 \cdot 10^{-3}\, eU_g$. For Al in Ref. 15 $\gamma_{\Sigma i} \sim 1$ at $U_g = 6$ kV, what is 1.4 times higher than for the ultrahigh vacuum (Fig. 4), but 40 times lower than needed for interpretation of the experiment.[24]

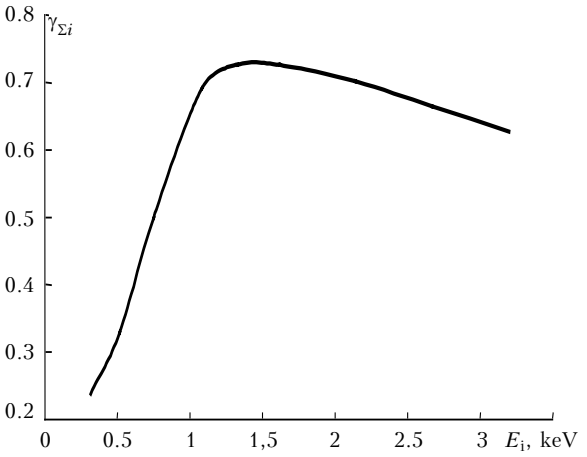

Fig. 4. Total electron yield as a function of the energy of ions and fast atoms at the voltage of 6 kV across the gap.

To increase $\gamma_{\Sigma i}$ in e-beam generators based on abnormal discharge, mixtures with O_2 additives are used to form the Al_2O_3 film of the optimal thickness and the highest $\gamma_{i,a}$ on the cathode surface.[17] Figure 5 shows the potential distribution (curve *1*) in the cathode region for such discharges (in Nl coordinates, l is the distance from the cathode),[64] as well as the potential distribution in OD (curve *2*) used in Ref. 52 to calculate $\gamma_{\Sigma i}$. It can be seen that for the conditions of Ref. 64 E/N and, consequently, the effective $\gamma_{\Sigma i}$ are higher than for the conditions of Ref. 52. However, in both cases, $\eta < 40\%$ (Refs. 17 and 65) (the value $\eta \sim 40\%$ in Refs. 17 and 65 corresponds to the higher current, temperature, and E/N than those, at which the potential distribution was measured in Ref. 64). Consequently, under the conditions of Refs. 17 and 65 and especially Ref. 52, $\gamma_{\Sigma i} < 0.7$, what is 60 times lower than needed for interpretation of the experiment.[24] The actual contribution of the emission under the effect of heavy particles to the total OD current is shown in the 15th column of Table 1 as calculated based on the current data on γ_i and γ_a and the measured η.

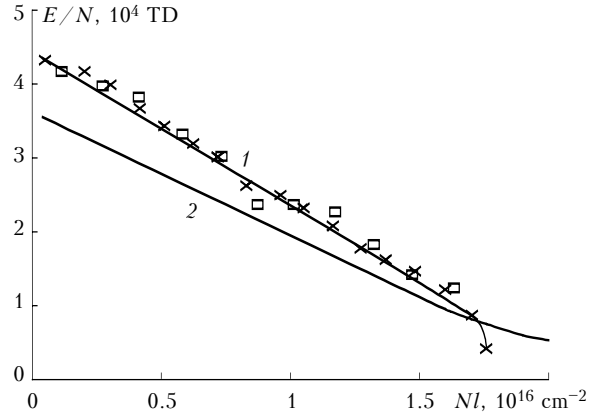

Fig. 5. Field strength distribution in abnormal discharge with e-beam[64] (*1*) and open discharge[21,52] (*2*), $p_{He} = 1.3$ (×) and 2.3 Torr ( ).

4. Volt-ampere characteristics and their evolution

Studying volt-ampere characteristics, their evolution, and dependence on the discharge geometry is very important for investigation of the open discharge mechanism. The pulsed and continuous modes of the discharge glow are now studied most thoroughly. The analysis of the literature data presented in Table 2 shows that in the both modes the VAC of the open discharge differs widely from the VAC of the abnormal discharge. The data on the experimental current density for OD j_g and calculated by Eq. (1) for abnormal discharge j_{ad} are given in Table 2 for different stages of the OD evolution: at the voltage $U_g(m)$ across the gap – when the current is maximal and at $U_g(0.5)$ – when the current is halved at the pulse trailing edge; for the continuous mode $U_g(m)$ is the constant voltage across the gap. For comparison, we also present the data on the current density in the classical abnormal discharge with e-beam from Refs. 18 and 65.

Table 2

#	He pressure, Torr	$U_g(m)$, kV	$U_g(0.5)$, kV	j_g, A/cm^2	j_{ad}, A/cm^2	$\frac{j_{ad}}{j_g}$	Ref.
			Continuous mode				
1	1	5	–	0.114	0.312	2.74	65
2	1	2.5	–	0.025	0.039	1.56	65
3	2.0	5.45	–	0.021	1.62	77	48
4	7.3	1.72	–	0.0015	0.68	453	t.p.
5	11	1.04	–	0.001	0.34	340	23
6*	9.6	0.63	–	0.00137	0.058	42	t.p.
			Pulsed mode				
7	3	2.38	–	0.425	0.303	0.71	18
8	20	7.8	–	45	475	10.6	21
9	20	–	5.1	22.5	132	5.9	21
10	40	4	–	60	256	4.3	7
11	40	4.8	–	37	442	11.9	21
12	40	–	3.9	19	237	12.5	21

* OD with artificial photoemission (see Fig. 1).

The VAC of the open discharge differs from the VAC of the abnormal discharge, as demonstrated in Table 2, first, because of different mechanisms of electron emission from the cathode. In view of the photoelectron character of the emission in the open discharge, the current in this discharge is always lower and depends on the size of the drift space and geometric transparency of the mesh. This was noted in all papers devoted to the open discharge investigation. For the pulsed open discharge, this effect was studied in detail in Ref. 25. In this paper, we present the data for continuous OD.

Figure 6*a* shows the dependence of the current density in the gap on the beam cross section area for the case when a part of the cathode is covered by a mica plate. The dashed curve here is for the dependence of the relative cathode irradiation on the area of its open part. It can be seen that as photoemission increases due to the cell geometry (2), the current density increases too, as in the pulsed discharge at variation of μ (Ref. 25). An interesting feature of the data shown in Fig. 6 is that not only the current density, but also the efficiency of e-beam generation significantly depend on the beam cross dimensions. This fact explicitly points to the photoelectron character of the emission under these conditions.

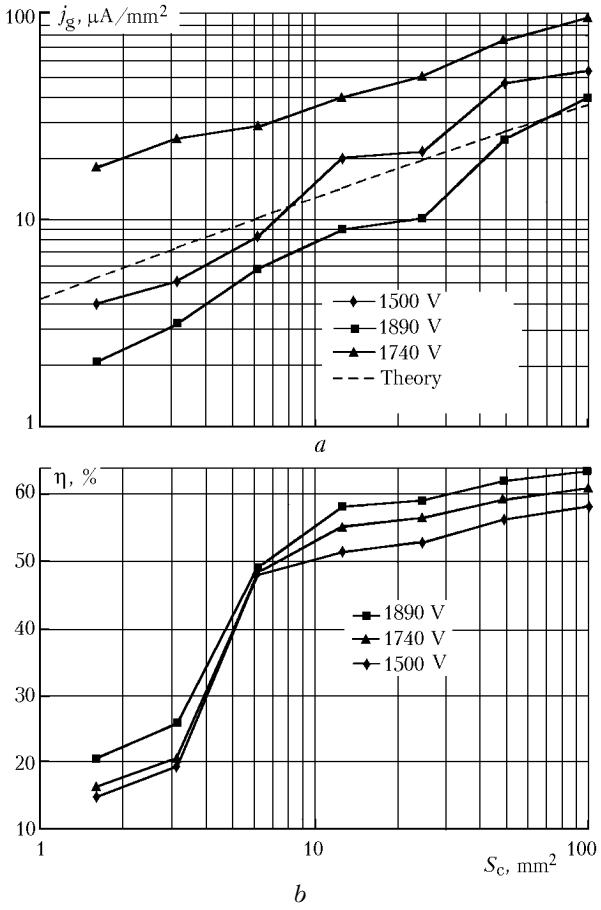

Fig. 6. Dependence of the current density (*a*) and e-beam generation efficiency (*b*) on the area of the cathode open part and voltage across the gap; p_{Ne} = 1.6 (■) and 2.6 Torr (▲, ♦).

The VAC under the quasi-continuous conditions was studied only in Ref. 10, where it was noted that as the pulse duration increases, the quasi-stationary stage of the open discharge is formed. The VAC in this open discharge obeys the law (1). Because of the importance of conclusions about the physical processes in OD which follow from Ref. 10 (for example, in Ref. 14), it is necessary to study the VAC of the quasi-stationary discharge. The results of such studies are presented below. In order to compare the results with the data of other authors, the measurements were conducted mostly with He as a working gas. The current ranged from 30 mA/cm^2 to 1 A/cm^2 at the rectangular pulse duration τ = 10 μs and to 10 A/cm^2 at τ = 1 μs, and the He pressure ranged from 16 to 30 Torr.

In Fig. 7 curves *1–3* are for the VAC of quasi-continuous discharge at different values of the He pressure close to the value optimal for OD glow and e-

beam generation, pl_g = 1.6–3 Torr·cm ($(pl_g)_{opt}$ = = 2 Torr·cm (Ref. 7)), and curve *4* is for the VAC of the abnormal discharge.[10] In the widest range of j variability – from 30 mA/cm^2 to 10 A/cm^2, the VAC was measured at p_{He} = 16 Torr. At the higher He pressure, the quasi-stationary phase of the discharge at high j cannot be obtained because of the exponential increase of the current even at R_b = 0.5 $k\Omega$. It can be seen from the figure that the VAC of the open discharge differs sharply from the VAC of the abnormal discharge both quantitatively and qualitatively. This difference decreases, as the He pressure increases. To be noted in the first turn is the absence of the law (1) for the VAC, that is, the VAC at every p is individual. Another interesting fact is the presence of bends on the open discharge VAC, which are determined by the complex dependence of the photoemission intensity on the excitation conditions.

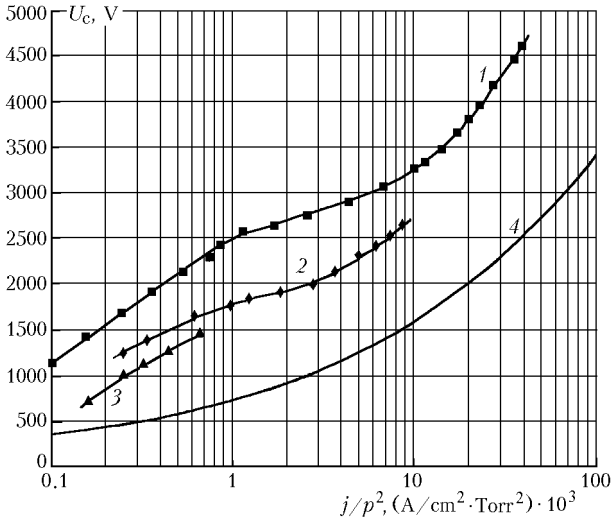

Fig. 7. Volt-ampere characteristics of the open (*1–3*) and abnormal (*4*) discharge; He pressure of 16, 24, 30 Torr (*1–3*); from Ref. 10 (*4*).

An unexpected discharge feature at high $j \geq 5$ A/cm^2 is that the current density decreases by the end of the pulse, while the voltage either stabilizes or even begins to increase. Two processes leading to the decrease of UV emission and, consequently, the current in the gap cause this decrease: (a) complete neutralization of induction and compensation currents, (b) electron quenching of He emitting states.

Since the electron emission is caused by photoemission, the VAC for OD should depend on the drift space geometry and the method of anode grounding[23] in both the continuous and pulsed modes. As an example, Fig. 8 shows how the relative current j/j_0 in the gap increases at the transition from S_c = 0.5 cm^2 to S_c = 1 cm^2 (curve *1*, τ = 10 μs, U_g varies from 0.875 to 3.16 kV, the first three points at low current are obtained for the continuous mode), as the length h of the drift space increases from 0.3 to 2 cm (curve *2*, τ = 2 μs, U_g = 1.87–3.46 kV) and at the transition from the circuit with the grounded anode to the anode with floating voltage (curve *3*, U_g = 1.43–2.52 kV, τ = 4 μs).

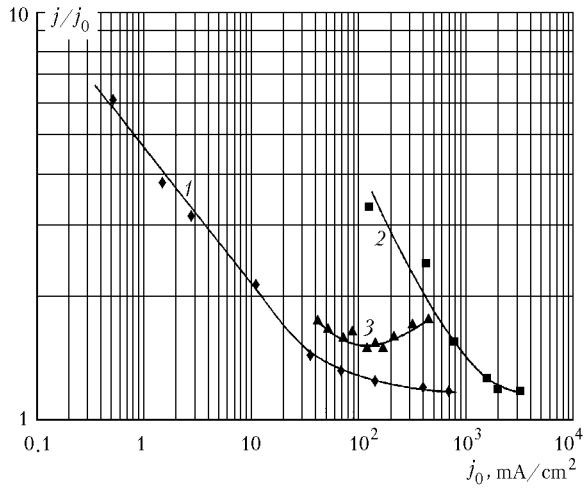

Fig. 8. Relative current increase j/j_0: p_{Ne} = 3.5 Torr, τ_p = 10 μs (*1*); p_{Ne} = 5.1 Torr, τ_p = 2 μs (*2*); p_{He} = 10 Torr, τ_p = 4 μs (*3*).

5. Discussion

The data presented in Sections 1–3 evidence that the open discharge differs considerably from the well-known abnormal discharge. In particular, direct experiments confirmed the main feature – photoelectron character of the open discharge that provides its capability of high-efficient e-beam generation at relatively low voltage (several kilowatts) and high He pressure (tens of Torrs). Below we discuss other features of the open discharge. The character of the potential distribution in the gap plays a very important role in the open discharge functioning. Since this issue was not considered above, it is worth beginning our discussion with it.

5.1. Potential distribution in the discharge gap, its evolution, and relationship with the e-beam generation efficiency

In Ref. 1, based on indirect evidence, it was assumed that the potential distribution in the accelerating gap is sharply inhomogeneous. Direct probing measurements[19] show that the CVD length at the current higher than 20 A/cm^2 is $l_0 \sim \lambda_c$. The polarization measurements conducted at the initial stage of a discharge at the maximal voltage amplitude[20] (for detail see Ref. 66) show that already in this case the field near the cathode is more than ten times stronger than that in the gap. Comparison of the data from Ref. 19 for the initial phase of a discharge with the data from Ref. 20 at the close current density demonstrates a rather close correlation. Klimenko and

Korolev[10] and Sorokin[14] hold the idea on the strong field nearby the cathode.

Somewhat opposite opinion was expressed in Ref. 21. It follows therefrom that even if the field is distorted, then only in the final phase of the discharge. The distortion at the maximal current and at the leading edge is so weak that the concept of CVD does not work. The differences are explained by the fact that when meshes are used as probes,[19] a sparking arises between them, therefore the measurements of Ref. 19 are incorrect. It should be noted that the assertion about sparking under the conditions of Ref. 19 is contrary to fact. On the contrary, systems with meshes under floating potential are highly stable in operation and used for obtaining e-beams with improved characteristics.[48]

The idea on weak distortion of the field in the gap conflicts with obtaining $\eta \sim \mu$ at the initial stage of discharge.[14,25] Actually, at weak distortion of the field it penetrates behind the mesh, thus distorting parallelism of force lines in the gap. This leads to distortion of the electron trajectory and interception of a significant part of e-beam by the mesh. The theory of this process is well developed in Ref. 22 and confirmed by experiments; this gives $I_a = 2I_e$ for the conditions of Ref. 14. Correspondingly, the theoretical value is $\eta_{max} = 0.33$, rather than $\eta = \mu$. Therefore, obtaining $\eta \sim \mu$ is impossible without revision of the results of Ref. 21.

It can be shown that the method used in Ref. 21 strongly overestimates the potential because of high capacity of probes and their weak electric coupling with the volume of the accelerating gap. As a result, the time constant of neutralization of the probe charge arising at voltage application is $\delta\tau_p > 160$ ns, what is far longer than the current pulse. Therefore, the probe potentials in Ref. 21 reflect, to a great extent, only the weakly perturbed evolution of the cathode voltage, rather than the actual distribution of $\varphi(x)$ in the gap. The actual field in the cathode region can be calculated from the following prerequisites.

Electrons generated in the gap leave it ~ 150 times faster than He^+ ions. Therefore, the increasing concentration of He^+ distorts the field, thus preventing the electron departure. Since $d_c/l_g \gg 1$, the field of ions can be calculated by the equation for charges uniformly distributed over a plane, namely, $E_x = \sigma_{yz}/2\varepsilon_0$, where σ_{yz} is the surface charge density and ε_0 is the permittivity of vacuum.

On the other hand, $\sigma_{yz} = E_g/\theta \int j(t)\, dt$, what leads to the following equation for the time constant of shielding of the applied field, i.e., if $\Delta E_x(\tau_0) = U_g/l_g$:

$$\tau_0 = 2\varepsilon_0 U_g S\theta / l_g \langle I_g \rangle E_g , \qquad (9)$$

where E_g is the energy loss of the electron beam in the gap; θ is the energy consumed for generation of one He^+ ion, $E_g/\theta = 0.41$ for $E_e = 6$ keV (Ref. 5).

Calculation by Eq. (9) gives $\tau_0 = 1.3$ ns at the maximal current, what is far smaller than the minimal time needed for an ion to cross the accelerating gap $\tau_{dr} = 16$ ns in the absence of field distortion in the gap under the conditions of Ref. 24. Consequently, the field distortion is rather large and it follows ion generation and accumulation in the gap. As a result, the spatial charge of ions completely shields the external field in the most part of the gap already at the discharge initial stage and strongly decelerates the ion drift beyond the CVD region, what leads to fast collapse of the applied field in the narrow cathode region.

Neglecting the ion departure to the cathode, $n_i = 1.61 \cdot 10^{12}$ ions with the total charge $q_{yz} = 2.58 \cdot 10^{-7}$ C are generated in the gap at the leading edge as the current peaks. The field strength of this charge is $E_x = 1.46 \cdot 10^8$ V/m, what is 12.4 times stronger than the initial one. As a result, $l_0 = l_g/12.4 = 4.03 \cdot 10^{-3}$ cm, or $l_0 = 3\lambda_c$ ($E_i \sim 2$ keV). Processing of the oscillograms shown in Fig. 3 gives the integral value $q_{yz}(i)$ of the charge gone to the cathode in the form of the ion current: $q_{yz}(i) = 0.54 \cdot 10^{-8}$ C or 2% of the total charge, what confirms experimentally the conclusion about the current magnitude in the gap. In Ref. 21, where the gap length was 2.4 times longer and the current was 1.2 times higher at $p_{He} = 4$ kPa, $\tau_0 = 0.45$ ns and the characteristic length $l_0 \sim 1.4 \cdot 10^{-3}$ cm $\sim \lambda_c$ ($E_i \sim 5$ keV).

Since the ion current beyond the CVD region is $j_{ig} \sim j_i$, the speed of the electron drift in the gap is $V_{dr} \sim j_{ig}/en_i \sim 2 \cdot 10^5$ cm/s. This speed corresponds to $E/N = 10^2$ TD (Ref. 30) or $U_g - U_c = 50$ V if $l_g - l_c = 0.5$ mm. Thus, unlike the measurements of Ref. 21, the field is almost completely concentrated in the CVD region. However, the residual field beyond the CVD is sufficient for the time of electron departure from the gap to be ~ 1 ns, what maintains the volume charge of ions.

Thus, the ion lag and the absence of the need in ions for OD appearance and evolution lead to strong distortion of the well-known inequality for the abnormal discharge: $pl_a \geq 0.37\, pl_n$. In dense open discharge $pl_0 \ll 0.37\, pl_n$. Similar distortions under the conditions of overvoltage across the discharge gap were noticed still in Refs. 46 and 67. In Ref. 46 at discharge in deuterium, $E/N = 3 \cdot 10^5$ TD, the current density was only $j = 0.22$ A/cm^2, and $l_a = 1.1$ cm as measured by the probe method ($p_{D_2} = 0.079$ Torr), what made up $l_a = 0.1\, l_n$. This value is even smaller than in the open discharge. The calculation by the method from Ref. 19 gives for this case: $l_0 = 1.48$ cm or $l_0 = 0.135\, l_n$.

The existence of the strong CVD in combination with photoemission from the cathode is the main feature of the open discharge that provides $\eta_{in} > 90\%$ in the continuous and quasi-stationary modes. In e-beam generators based on abnormal discharge, close, but still less than 90%, values of η_{in} are achieved only at very low working pressure (usually less than 0.1 Torr) and high voltage ($U > 50$ kV) (Ref. 46) or with the use of specialized cathodes with increased

emission (Refs. 15 and 17). At $p_{He} = 1$ Torr, η_{in} is less than 80%, and with allowance for gas heating it is less than 50% at already reduced to the room temperature $p_{He} \sim 0.3$ Torr (Refs. 17 and 64).

Even higher values of η_{in} in OD (> 95%) can be achieved in the pulsed mode at the stage of growth and at the maximal current. The mechanism of obtaining so high η_{in} is closely connected with the short length of the CVD region and the ion lag restricting the ion drift to the cathode from the region of reduced field. When calculating η by the method from Ref. 19, due to small thickness of the cathode layer, wherefrom ions come to the cathode, the energy loss approximation[5] is incorrect, because the probability of repeated ionization in the CVD region by scattered and secondary electrons $P_{2i} \sim P_i^2$ is far lower than that by primary electrons P_i. Therefore, it was calculated based on the known dependence of the cross section of He ionization by electrons[68,69] and the character of potential distribution in the gap according to measurements of Ref. 19. The length $l_0 = 4.03 \cdot 10^{-3}$ cm corresponds to $U_c = 0.9\ U_{c0}$, where $U_{c0} \sim U_g$ is the total CVD value. Under these conditions, $P_i = 3.3 \cdot 10^{-2}$, at which the ion current at the cathode $j_i = 0.033\ j_e$ and the efficiency $\eta_{in} = 0.967$, what well agrees with the experimental data ($\eta_{in} = 0.976$).

At the same time, the reports on obtaining $\eta \sim \mu$ (Ref. 24) and even $\eta \sim 1$, that is, higher than μ (Refs. 13 and 14) should be considered with all due care. The mechanism of obtaining such phantom η is well-known[22] and caused by parasitic currents due to inelastic scattering and secondary electron emission from the anode. These processes can be neutralized by strong CVD and rather high pressure of the working gas.

5.2. Mechanism of electron emission and discharge VAC

In the well known papers, for example, Refs. 10 and 14, where it is believed that the open discharge is a sort of well-known abnormal discharge and, consequently, emission is induced by heavy particles, the presented evidence is indirect and based on the study of VAC under various conditions. The only paper, in which an attempt was undertaken to calculate $\gamma_{\Sigma i}$, is Ref. 52. It was shown above that $\gamma_{\Sigma i} < 0.7$ under the conditions of Ref. 52. Direct measurements of the ratio $I_e/I_i = 6.6$ at $U = 80$ kV and $p_{D_2} = 0.08$ Torr in Ref. 46 and at $\eta_{in} < 87\%$ in Ref. 15 in technological vacuum at the working gas pressure of 0.035 Torr indicate that the ratios $I_e/I_i = 10$ and, especially, $I_e/I_i = 41$ are unachievable at the ion-electron mechanism of emission. Therefore, in this paper, we discuss only indirect evidence used in Refs. 10 and 12–14.

The statement on the identity of open and abnormal discharges is based on the results of VAC measurements[10] under the conditions given in Table 3. Table 3 presents also the optimal and boundary conditions for existence of e-beam and open discharge from our pioneering paper.[7] It can be seen that VAC in Ref. 10 was measured in two limiting regions: either at very high pressures, where the threshold conditions on E/N for OD are not fulfilled, or at very low pressure, where OD is impossible because of weak self-irradiation. The actual VAC of the quasi-stationary OD under optimal conditions is far more complex (see Fig. 7), and, in the first turn, similarity laws like the law (1) do not exist for it.[15,46,67] The VACs in open and abnormal discharges differ dramatically for the continuous mode (see Table 2). Consequently, the conclusion[10–14] on the identity of abnormal and open discharges following from the similarity of VAC is unjustified.

5.3. VAC evolution and dependence on discharge geometry

Using the above results, we consider the OD properties, which are treated in Refs. 12–14 as unexplainable from the viewpoint of the photoelectron mechanism of emission and therefore the latter should be rejected.

1. Analyzing oscillograms of Ref. 24 (see Fig. 3 in this paper), Sorokin in Ref. 12 noticed that as the voltage decreases from 6 kV (maximum of the e-beam current) to 3 kV, the e-beam current should increase due to the increase of dE/dx, rather than decrease sharply as observed in the experiment. Therefore, Sorokin concludes that OD cannot have the photoelectron origin.

Table 3

#	Symbol on the plot	Pd, Torr · cm	U_c range, kV	E/N range, 10^3 TD	Reference
1	+	36.4	0.83...1.79	0.06...0.149	10
2	▲	18.2	1.02...2.32	0.168...0.36	
3	○	7.0	1.83...4.92	0.74...1.98	
4	●	0.49	1.91...4.01	11...23	
5	4	2.0	1.83...2.62	2.6...3.7	
6	5	1.0	–	–	
7	Δ	0.49	4.85...6.05	28...35	
8	□	0.28	5.5...6.75	55...67.5	
9	–	2.0 (opt.)	4.0	5.6	7
9′	–	2.8 (beam disruption)	3.2	4.5	

At least three mechanisms favor the decrease of the current: (a) disappearance of photoemission connected with field sagging in the drift space; (b) complete neutralization of induction and compensation currents; (c) quenching of resonance and other emitting He atomic states by secondary and discharge electrons accumulated by that time in the drift space ($n_e \sim 5 \cdot 10^{14}$ cm^{-3}). From Table 1 (rows 5 and 5′ corresponding to this example) it can be seen that the total emission due to excitation in the sagged field (pulse beginning) and the current generated in the drift space (pulse front) is an order of magnitude higher than that due to direct beam energy loss. Consequently, Sorokin in Ref. 12 considered only one of minor mechanisms of VUV radiation generation, which only slightly affects the VAC evolution.

2. In Refs. 13 and 14 it is stated that in the case of the photoelectron mechanism of electron emission in OD the discharge current in the quasi-stationary mode, once appeared, should inevitably achieve the value of the current in the vacuum diode. The actual current density in OD is four orders of magnitude lower. Therefore, Sorokin concludes[13,14] that the current in OD cannot have the photoelectron origin.

Let us consider this statement in more detail. First, the current in the gas-filled diode should not be the same as in the vacuum diode. For example, it follows from Fig. 1 that at $l_g = 1$ mm and $U_g = 6$ V at $p_{He} = 15.5$ Torr, the current is $j_g = 23$ μA/cm^2, what is more than two orders of magnitude lower than in the vacuum diode (3.44 mA/cm^2). As expected, the difference increases with the increasing He pressure. Second, in the case of Ref. 14 there is an efficient mechanism for OD self-stabilization. As follows from row 7 of Table 1, the emission mostly originates from the sagged field region. As a result, the increase of the current, to the contrary, decreases the emission because of the decrease of l_0 and field sagging behind the anode, and therefore it can be achieved only at increasing U_g.

Under the conditions, when the role of the sagged field is small, without application of ballast resistance at rectangular power supply pulses, the quasi-stationary mode cannot be achieved as was mentioned above. However, this OD instability is especially pronounced in the continuous mode. It can be seen from Fig. 2 (curve *2*) that the artificial increase of the energy pumped into the drift space by 40% leads to the 200% increase of the current. The extra contribution is due to the region remote from the cathode, where its efficiency is halved because of the geometric factor. Besides, the drift space provides for ~60% of the total power of emission (row 3 of Table 1). It follows herefrom that ~13% of change in the intensity of cathode photoemission from the drift space initiates threefold increase of the OD current. Even stronger effect takes place at the low intensity of emission, when self-stabilization caused by the gas heating is stronger. In this case $\Delta(I_g/I_{g0}) \sim 60\ \Delta(P_d/P_{e0})$. Consequently, OD is actually unstable, what agrees with its photoelectron origin.

3. In Ref. 14, as the length of the discharge gap increased from 1 to 4 mm, the current increased by an order of magnitude, what, in Sorokin's opinion, does not fit in the photoelectron mechanism. The data of Table 1 (rows 7, 7′) indicate that the contributions of the mechanisms γ_{p3}, γ_{p5}, and γ_{p6} changed totally as a result of this operation. This led to the change of $\gamma_{\Sigma p}$ and VAC. Redistribution of the main part of photoemission in favor of the γ_{p6} mechanism at $l_g = 4$ mm inevitably caused intensification of ionization processes in the gap, increase of j_i and total current, and, as a consequence, to drastic decrease of η. As a result, Sorokin[14] realized the discharge transition from open to abnormal (known from Ref. 19) through the increase of the discharge gap length with all the corresponding consequences.

4. In Ref. 14, as the length of the drift space increased from 2 to 30 mm, no marked changes were found in the total current, what, in Sorokin's opinion, is also unexplainable from the viewpoint of the photoelectron mechanism. The results of analysis of this example are given in rows 7 and 7′ of Table 1. They demonstrate that these changes should not take place, since the fraction of γ_{p1}, a single one depending on h, is actually small and makes up ~0.1 of $\gamma_{\Sigma p}$.

Thus, the main features of the VAC in OD can be easily interpreted from the viewpoint of the photoelectron mechanism.

Conclusions

1. The photoelectron origin of the open discharge is confirmed by direct experiments and estimation of the number of electrons emitted from the cathode under the exposure to VUV radiation generated at deceleration of one electron.

2. Electron emission under the effect of heavy particles cannot provide both the self-sustaining character of the open discharge and the high, about the geometrical transparence of the anode mesh, efficiency of e-beam generation. The difference between the number of electrons emitted under the effect of heavy particles and that actually realized in OD is so large (up to two orders of magnitude) that it cannot be explained by experimental errors.

3. The volt-ampere characteristics of OD in all modes of its glow differ widely from the VAC of the abnormal discharge. The difference in the current density depends on the discharge geometry and can exceed two orders of magnitude.

4. The field in the gap in the dense stage of OD ($j > 1$ A/cm^2) is concentrated in an extremely narrow cathode region, whose length can be much smaller than the limit CVD length of abnormal discharge, up to the ion mean free path. The comparable field distortion

occurs also in discharges of other types with high-efficiency e-beam generation.

5. The OD capability of e-beam generation with $\eta_{in} > 90\%$ at the increased, as compared with abnormal discharge, pressure of the working gas is intimately linked with its photoelectron nature and strong distortion of the field in the discharge gap.

6. A consistent explanation to all phenomena in OD is given from the viewpoint of the photoelectron mechanism, although earlier it was considered impossible.

7. A set of OD characteristics established reliably by now shows that the open discharge possesses some features, which do not allow it to be assigned to some known sort of gas discharge.

The consistent use of the obtained results allowed us to realize the practical efficiency of e-beam generation in the open discharge $\eta = 99.8\%$ (Ref. 70).

References

1. P.A. Bokhan and A.R. Sorokin, Zh. Tekh. Fiz. **55**, No. 1, 88–95 (1985).
2. P.A. Bokhan, Kvant. Elektron. **13**, No. 9, 1837–1846 (1986).
3. Yu.V. Koptev, E.L. Latush, and M.F. Sem, Kvant. Elektron. **17**, No. 4, 412–413 (1990).
4. P.A. Bokhan and A.R. Sorokin, Opt. and Quantum Electron. **23**, No. 4, 523–538 (1991).
5. S.V. Arlantsev, B.L. Borovich, V.V. Buchanov, E.I. Molodykh, and N.I. Yurchenko, J. Russ. Las. Res. **16**, No. 2, 99–119 (1995).
6. P.A. Bokhan and G.V. Kolbychev, Pis'ma Zh. Tekh. Fiz. **6**, No. 7, 418–421 (1980).
7. P.A. Bokhan and G.V. Kolbychev, Zh. Tekh. Fiz. **51**, No. 9, 1823–1831 (1981).
8. A.R. Sorokin, "*Study of new methods for excitation of gas-discharge high- and medium-pressure lasers*," Author's Abstract of Doct. Phys.-Math. Sci. Dissert., Novosibirsk (1999), 54 pp.
9. G.V. Kolbychev and B.A. Samyshkin, Zh. Tekh. Fiz. **51**, No. 10, 2031–2037 (1981).
10. K.A. Klimenko and Yu.D. Korolev, Zh. Tekh. Fiz. **60**, No. 9, 138–142 (1990).
11. A.R. Sorokin, Pis'ma Zh. Tekh. Fiz. **21**, No. 17, 33–37 (1995).
12. A.R. Sorokin, Pis'ma Zh. Tekh. Fiz. **21**, No. 20, 37–40 (1995).
13. A.R. Sorokin, Pis'ma Zh. Tekh. Fiz. **22**, No. 13, 17–21 (1996).
14. A.R. Sorokin, Zh. Tekh. Fiz. **68**, No. 3, 33–38 (1998).
15. M.A. Zav'yalov, Yu.E. Kreindel', A.A. Novikov, et al., *Plasma Processes in Technological Electron Guns* (Energoatomizdat, Moscow, 1989), 256 pp.
16. G.V. Kolbychev and I.V. Ptashnik, Pis'ma Zh. Tekh. Fiz. **11**, No. 8, 1106–1110 (1985).
17. J.J. Rocca, J.D. Meyer, M.R. Farell, and G.J. Collins, J. Appl. Phys. **56**, No. 3, 790–797 (1984).
18. S. Wernsman, H.F. Fanea-Sandoval, J.J. Rocca, and H. Manoini, IEEE Trans. Plasma Sci. **PS-14**, No. 4, 47–51 (1986).
19. P.A. Bokhan, Zh. Tekh. Fiz. **61**, No. 6, 61–68 (1991).
20. V.P. Demkin, B.V. Korolev, and S.V. Mel'nichuk, Fiz. Plazmy **21**, No. 1, 81–84 (1995).
21. G.V. Kolbychev and I.V. Ptashnik, Atmos. Oceanic Opt. **12**, No. 11, 1020–1024 (1999).
22. B.M. Tsarev, *Calculation and Design of Electron Lamps* (Energiya, Moscow, 1967), 671 pp.
23. A.P. Bokhan and P.A. Bokhan, Pis'ma Zh. Tekh. Fiz. **27**, No. 6, 7–12 (2001).
24. G.V. Kolbychev, Atmos. Oceanic Opt. **6**, No. 6, 375–382 (1993).
25. G.V. Kolbychev and I.V. Ptashnik, Pis'ma Zh. Tekh. Fiz. **59**, No. 9, 104–110 (1989).
26. A.V. Gurevich, Zh. Eksp. Teor. Fiz. **39**, No. 5(11), 1296–1307 (1960).
27. A.M. Kol'chuzhkin and V.V. Uchaikin, *Introduction to Theory of Particle Propagation through Matter* (Atomizdat, Moscow, 1978), 255 pp.
28. L.A. La Verne and A. Mozumder, J. Phys. Chem. **89**, No. 20, 4219–4225 (1985).
29. Yu.N. Sytsko and S.I. Yakovlenko, Fiz. Plazmy **2**, No. 1, 63–71 (1976).
30. H. Helm, J. Phys. B **10**, No. 18, 3683–3697 (1977).
31. G.V. Kolbychev, Izv. Vyssh. Uchebn. Zaved., Ser. Fiz., No. 11, 84–86 (1999).
32. N.S. Grigor'ev and E.Z. Meilikhov, eds., *Physical Constants* (Energoatomizdat, Moscow, 1991), 1232 pp.
33. A.N. Zaidel' and E.Ya. Shreider, *Vacuum Spectroscopy and Its Applications* (Nauka, Moscow, 1976), 431 pp.
34. R.B. Cairns and J.A.R. Samson, J. Opt. Soc. Am. **56**, No. 11, 1568–1573 (1966).
35. W.C. Walker, O. P. Rustgio, and G.L. Weissler, J. Opt. Soc. Am. **49**, No. 5, 471–475 (1959).
36. M. Krumrey, E. Tegeler, J. Barth, M. Krisch, F. Schäfers, and R. Wolf, Appl. Opt. **27**, No. 20, 4336–4341 (1988).
37. B. L. Henke, J.P. Knauer, and K. Premarante, J. Appl. Phys. **52**, No. 3, 1509–1520 (1981).
38. D. Hasselkamp, in: *Particle Induced Electron Emission II*, ed. by G. Höhler, Springer Tracts. Mod. Phys. **123**, 1–95 (1992).
39. I.N. Evdokimov, E.S. Mashkova, V.A. Molchanov, and D.D. Odintsov, Phys. Status. Solidi. A **9**, No. 2, 407–415 (1967).
40. G.M. Petrov, T. Petrova, and A.B. Blagoev, Appl. Phys. Lett. **77**, No. 1, 40–42 (2000).
41. P.A. Bokhan and G.V. Kolbychev, Zh. Tekh. Fiz. **51**, No. 9, 1823–1831 (1981).
42. P.A. Bokhan and A.R. Sorokin, Zh. Tekh. Fiz. **55**, No. 6, 1168–1170 (1985).
43. M. Rösler and W. Brauer, in: *Particle Induced Electron Emission I*, ed. by G. Höhler, Springer Tracts. Mod. Phys. **122** (Springer-Verlag, Berlin, 1991), pp. 1–65.
44. J. Devooght, J.C. Dehaes, A. Dubus, M. Cailler, and J.-P. Ganachayd, in: *Particle Induced Electron Emission I*, ed. by G. Höhler, Springer Tracts. Mod. Phys. **122** (Springer-Verlag, Berlin, 1991), pp. 67–128.
45. I.K. Kikoin, ed., *Tables of Physical Constants* (Atomizdat, Moscow, 1976), 1006 pp.
46. G.W. McClure, Phys. Rev. **124**, No. 4, 969–982 (1961).
47. P.A. Bokhan and A.R. Sorokin, Pis'ma Zh. Tekh. Fiz. **8**, No. 15, 947–950 (1982).
48. A.R. Sorokin, Zh. Tekh. Fiz. **65**, No. 5, 198–201 (1995).
49. V.L. Granovskii, *Electrical Current in Plasma* (Nauka, Moscow, 1971), 543 pp.
50. R.A. Baragiola, E.V. Alonso, and A.O. Florio, Phys. Rev. B **19**, No. 1, 121–129 (1979).
51. Yu.P. Raizer, *Gas Discharge Physics* (Nauka, Moscow, 1987), 591 pp.

52. A.R. Sorokin, Pis'ma Zh. Tekh. Fiz. **26**, No. 24, 89–94 (2000).
53. R.A. Baragiola, E.V. Alonso, J. Ferron, and A. Oliva-Floria, Surface Sci. **90**, 240–255 (1979).
54. P. Varga and H. Winter, in: *Particle Induced Electron Emission II*, ed. by G. Höhler, Springer Tracts. Mod. Phys. **123**, 149–215 (1992).
55. G. Lakits, F. Aumayr, M. Heim, and H. Winter, Phys. Rev. A **42**, No. 9, 5780–5783 (1990).
56. G. Lakits, A. Arnau, and H. Winter, Phys. Rev. B **42**, No. 1, 15–24 (1990).
57. I. Amdur and H.J. Pearlman, Chem. Phys. **9**, 503–506 (1941).
58. I. Amdur and A.L. Harkness, J. Chem. Phys. **22**, No. 4, 664–669 (1954).
59. E.W. McDaniel, *Collision Phenomena in Ionized Gases* (Wiley, New York, 1964).
60. H.W. Berry, Phys. Rev. **99**, No. 2, 553–555 (1955).
61. H.C. Hayden and N.G. Utterback, Phys. Rev. A **135**, No. 6, 1575–1579 (1964).
62. G.V. Kolbychev and I.V. Ptashnik, Atmos. Oceanic Opt. **13**, No. 3, 243–247 (2000).
63. A. Baragiola, in: *Low Energy Ion-Surface Interaction*, ed. by J.W. Rabalias, (Wiley, New-York, 1994), Chap. 4, pp. 188–261.
64. S.A. Lee, L.U.A. Andersen, J.J. Rocca, M. Marconi, and N.D. Reesor, Appl. Phys. Lett. **51**, No. 6, 409–411 (1987).
65. J.J. Rocca, J.D. Meyer, Z. Yu, M. Farrell, and G.J. Collins, Appl. Phys. Lett. **41(9)**, 811–813 (1982).
66. V.P. Demkin, "*Polarization of Stark atomic states and methods of polarization spectroscopy of plasma in electric field*," Doct. Phys.-Math. Dissert., Tomsk (1995), 242 pp.
67. M. Nahemov and N. Wainfan, J. Appl. Phys. **34**, No. 10, 2988–2992 (1963).
68. J.H. Miller and S.T. Manson, Phys. Rev. A **29**, No. 5, 2435–2439 (1984).
69. G. Garcia, F. Arqueras, and J. Campos, J. Phys. B **19**, No. 22, 3777–3785 (1986).
70. P.A. Bokhan and D.E. Zakrevskii, Pis'ma Zh. Tekh. Fiz. (in print).